We are IntechOpen,
the world's leading publisher of
Open Access books
Built by scientists, for scientists

6,900
Open access books available

185,000
International authors and editors

200M
Downloads

154
Countries delivered to

Our authors are among the

TOP 1%
most cited scientists

12.2%
Contributors from top 500 universities

BOOK CITATION INDEX
CLARIVATE ANALYTICS
INDEXED

WEB OF SCIENCE™

Selection of our books indexed in the Book Citation Index
in Web of Science™ Core Collection (BKCI)

Interested in publishing with us?
Contact book.department@intechopen.com

Mass Transfer Mechanisms and Transport Resistances in Membrane Separation Process

Amira Abdelrasoul, Huu Doan, Ali Lohi and
Chil-Hung Cheng

Additional information is available at the end of the chapter

Abstract

One of the major obstacles preventing a more widespread application of membrane technology is the fact that the filtration performance inevitably decreases with filtration time. The understanding of causes of flux decline and the ability of predicting the flux performance is crucial for more extensive membrane applications. Therefore, this review focused on the analysis of the interrelated dynamics of membrane fouling and mass transport in the filtration/separation process. Furthermore, findings from various studies undertaken by many researchers to investigate various aspects of these complex phenomena, were analyzed and discussed. These previous studies form the foundation essential for the alleviation of adverse effect of membrane fouling and emphasize the fact that the development of a complex overlapping approach is needed. Investigations of the mechanisms of mass transfer in low and high pressure membranes, analyses of diffusion mechanisms in the membrane pore together with identifications of transport resistances resulting from membrane fouling will allow for a comprehensive understanding and in-depth knowledge of the fouling phenomenon and applicable mass transfer mechanisms.

Keywords: mass transfer, modeling, diffusion, boundary layer, transport resistances, membrane fouling

1. Introduction

Today membrane technology is considered an important tool for sustainable growth in the industry due to its simplicity in concept and operation, modularity for an easy scale-up, potential to reclaim both permeate and retentate for recycling purposes, and reduced energy demand, all of which make it attractive for a more rational utilization of raw materials and waste minimization. Various membrane operations are currently available for a wide spectrum of industrial applications, where most of them can be used as unit operations in pressure driven processes, such as: microfiltration (MF), ultrafiltration (UF), nanofiltration (NF), reverse osmosis (RO), and membrane distillation (MD). Membrane operations show potential in molecular separation, clarification, fractionation, and concentration in liquid and gas phases. Nevertheless, one of the major obstacles preventing a more widespread application of membrane technology is the fact that the filtration performance inevitably decreases with filtration time. This phenomenon is known as membrane fouling and is considered to be the most serious problem affecting system performance and the primary challenge in membrane development. As such, membrane fouling leads to lower mass transfer rate, higher operating cost, higher energy demand, reduced membrane life time, and increased cleaning frequency.

The reduction of membrane flux below that of the corresponding pure water flux, or more generally, pure solvent flux can be divided into two separate components. First, the concentration polarization, which is a natural consequence of the membrane's selectivity [1]. This phenomenon leads to an accumulation of particles or solutes in a mass transfer boundary layer adjacent to the membrane surface. The dissolved molecules accumulating at the surface hinder the solvent transport, which in turn lowers the solvent flow through the membrane. Second, due to the blockage of membrane pores during the filtration process by the combination of sieving and adsorption of particulates and compounds onto the membrane internal surface or within the membrane pores. During this process additional hydraulic resistance is added to the permeate flux. Fouling leads to an increase in resistance, resulting in less flux for a given transmembrane pressure (TMP), or a higher TMP if flux is kept invariant [2]. Understanding the concentration polarization resistance is important when attempting to distinguish a reduction in the driving force across the membrane from the increase in resistance due to the fouling of the membrane [3, 4]. As the material passes through the membrane, it has to be transferred to the surface, diffused through the membrane, and finally transfered from the other side of the membrane to the bulk phase. When the material dissolves within the membrane, then the components are in equilibrium at the surfaces corresponding to their solubility in the membrane. The solute mass transfer through the membranes is controlled by diffusion as a result of the concentration gradient across the membrane surface. In our previously developed mechanistic model for membrane fouling, the mass of fouling attached to the pore wall was a function of the mass transfer coefficient, which, in turn, was dependent on the diffusion coefficient of the foulants in water, particle sizes, and membrane pore sizes [5, 6].

Researchers have invested a lot of effort in seeking new accurate models for the prediction of membrane performance. In most applications, the system equations were derived based on simplifications and assumptions, which resulted in limited practical application of these models.

Nevertheless, these models provide sufficient basis for an incorporation of more parameters for more realistic scenarios. While so far no universally accepted model exists for describing diffusion-controlled membrane processes, understanding the multiple factors affecting membrane mass transfer would certainly help to develop better predictive models. There are many different theories and models describing mass transfer in diffusion-controlled membrane processes, however, several fundamental principles or theories are used as the basis for the majority of these models: convection, diffusion, film theory, and electroneutrality [7, 8]. Most mass transport models assume constant mass transfer coefficients (MTCs) based on a homogeneous membrane surface. Recent innovative studies evaluated mass transfer processes by incorporating membrane surface morphology into a diffusion-based model while assuming that MTCs are dependent on the thickness variation of the membrane's active layer [9]. A non-homogeneous diffusion model (NHDM) was then developed in order to account for the surface variations in the active layer [10]. Notably, concentration polarization (CP) is also affected by this non-homogeneous surface property. As a consequence, the NHDM was modified by incorporating the CP factor. Recent studies have likewise shown that the membrane surface morphology influences colloidal fouling behavior. Therefore, the main objectives of this chapter are to investigate the mechanisms of mass transfer, to critically analyze the different diffusion mechanisms in membrane pores, to identify different transport resistances resulting from membrane fouling, and to discuss various models of mass transfer, in order to obtain a comprehensive understanding of the factors affecting mass transfer phenomenon in membrane and help to develop a comprehensive model predicting the membrane performance.

2. Mass transfer and modeling of the filtration process in the absence of fouling

For an in-depth analysis of the transport resistances in the filtration/separation process due to membrane fouling, it is necessary to understand the mass transfer occurring through membranes in the absence of fouling. This type of transport in membranes can be generally classified into two types of diffusion: first is the diffusion through a dense membrane, which follows the Fick's law and does not depend primarily on the structure of the solid membrane; and second is the diffusion in porous membrane where the porous structure and channel type are important. This study will briefly consider both types of this diffusion.

2.1. Solution diffusion theory through dense membranes

The solution-diffusion process, as illustrated in Figure 1, is the most common mechanism for mass transport through nonporous membranes [11]. It is generally suggested that the component permeation through a homogeneous membrane consists of five fundamental mutually dependent processes: (1) the solute molecules must first be transported or diffused through the liquid film (or gas film; in the later case the mass transfer resistance of the boundary layer is negligible causing this step to be omitted) of the feed phase on the feed side of the membrane, as shown in Figure 1 (B); (2) the solution of the solute molecule in the upstream surface of the

membrane; (3) diffusion of the dissolved species across the membrane matrix occurs; (4) desorption of the solute molecules in the downstream side (permeate side) of the membrane; and (5) diffusion through the boundary layer of the permeate phase. The first and the fifth steps can be omitted when there are insignificant mass transfer resistances between the liquid and membrane phases. This assumption is valid for gas permeation or liquid permeation with high flow rates in the fluid phases on both sides of the membranes.
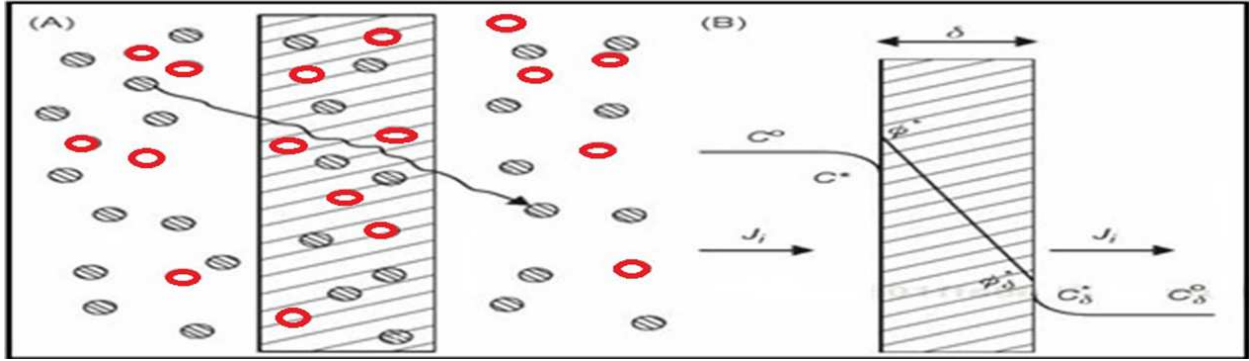
Figure 1. (A) Mass transport through dense membrane (B) Concentration Profile

Fick's first law relates the diffusive flux to the concentration under the assumption of steady state. It postulates that the flux goes from regions of high concentration to regions of low concentration, with a magnitude that is proportional to the concentration gradient [12]. Fick's first law of diffusion is mathematically expressed in Equation (1):

$$J = -D\frac{dC}{dZ} \tag{1}$$

where J is the rate of transfer per unit area of the membrane, C is the concentration of diffusing substances, and Z is the space coordinate measured normal to the membrane.

2.2. Convective transport through a porous membrane layer

As the basis of the pore flow model, pressure-driven convective flow is most commonly used to describe the flow in capillary tubes. The key mechanism at the core of both microfiltration and ultrafiltration is the sieving process, which effectively rejects molecules with the size greater than that of the membrane's pores. Commonly, two approaches are utilized as a way of describing permeability through porous membranes. In the first case, when the membrane resembles an arrangement of near-spherical particles, then the Carman–Kozeny equation can be applied [12], as illustrated in Equation (2):

$$J = \frac{\varepsilon^3}{K.\mu.S^2(1-\varepsilon)^2} \cdot \frac{\Delta p}{l_{pore}} \tag{2}$$

where J is the permeate flux, ε is surface porosity, μ is the dynamic viscosity of the permeate, K is a constant, l_{pore} is the thickness of the porous layer, ΔP is the pressure drop, and S is the specific area per unit volume. Both K and S depend upon the nature of the membrane porous structure. The permeability constant, K, is a function of the membrane structure, including characteristics such as pore size distribution, and porosity of the membrane, as well as the viscosity of the permeate.

In the second approach, the laminar fluid flow through the capillaries can be described by means of the differential momentum balance equation, Newton's law of viscosity [13, 14]. After integration, the well-known Hagen-Poiseuille equation for the average convective velocity through the porous membrane was obtained to calculate the permeate flux, as described by Equation (3):

$$ J = \frac{\varepsilon.\, d_{pore}^2}{32.\, \mu.\, \tau} \cdot \frac{\Delta p}{l_{pore}} \tag{3} $$

where τ is the tortuosity of the capillaries and d_{pore} is the diameter of the capillaries. Once again the flux is inversely proportional to the viscosity of the permeate. In addition, for the porous medium, Darcy law is the basic equation that can be utilized in order to describe the rate of fluid flow and thus allowing calculating the membrane area for a targeted separation at given conditions [12], as showed in Equation 4:

$$ Q = \frac{-k\,A}{\mu} \cdot \frac{\left(P_b - P_a \right)}{L} \tag{4} $$

where Q is the total discharge, [m³/s], k [m²] is the empirical constant representing permeability of the medium, (A) [m²] is the cross-sectional area to flow, $(P_b - P_a)$ is the pressure drop, μ [kg/(m s) or Pa s] is the viscosity, and L [m] is the membrane thickness.

3. Mass transfer boundary layer and membrane fouling

The rejection of contaminated particles results in a higher concentration in the mass transfer boundary layer. The process of mass accumulation in the mass transfer boundary region is called concentration polarization (CP). CP is a natural consequence of membrane selectivity, which leads to a reduction in the permeate flux because of the gel layer formation [15]. As a result of the high concentration of the rejected component, a back-diffusion occurs from the thin layer adjacent to the membrane back into the bulk [16], as shown in Figure 2. The reduction of membrane performance can be represented as a reduction in the effective TMP driving force due to an osmotic pressure difference between the filtrate and the feed solution immediately adjacent to the membrane surface [11]. As shown in Figure (2), $J_{1,\,con}$, $J_{2,\,con}$, and $J_{2,\,diff}$ [kmol/

m^2.s] represent the convective flux of the solution, the convective flux of the solute, and the diffusion flux of the solute, respectively. The following assumptions were made in order to obtain a mass balance on the feed side of the membrane: steady state, Fickian diffusion, the absence of chemical reaction, negligible concentration gradient parallel to the membrane, and constant density and diffusion coefficient independent of solute concentration [17]. Therefore, the net flux of the solute is the difference between the convective flux and back diffusion flux of the solute.
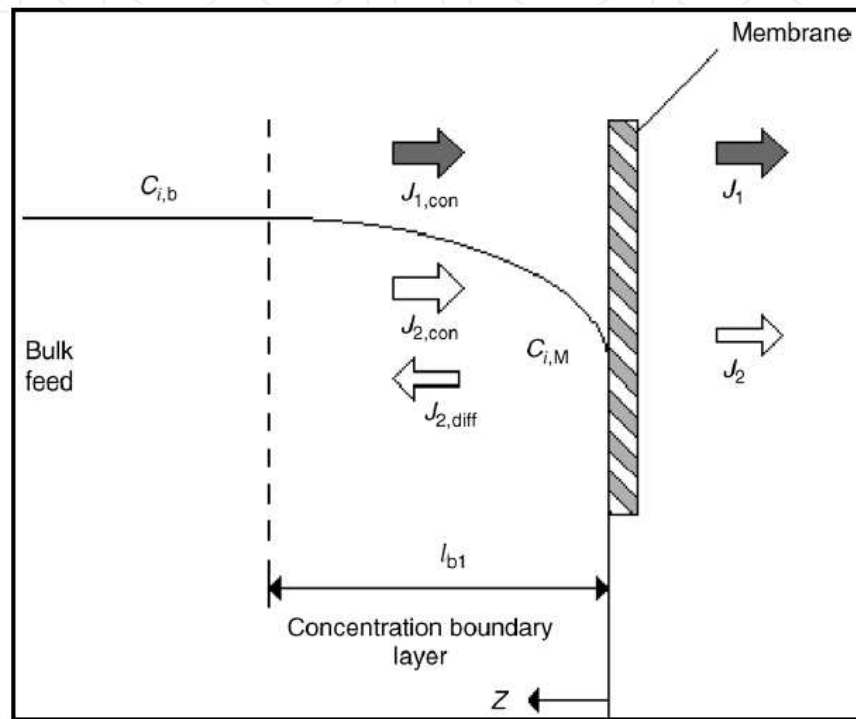
Figure 2. Schematic diagram of concentration polarization

Thus, in general the overall mass balance equation of a component i can be written as:

$$J. \, C_i = J. \, C_{i,p} - D_{ji} \frac{dC_i}{dZ} \tag{5}$$

where J is the volumetric permeate flux, C_i is the concentration of solute i. D_{ji} is the diffusivity of component i, and l_{bl} is the thickness of the mass transfer boundary layer [18]. Integration of Equation (5) gives the well-known polarization equation as below:

$$\left(C_{i,M} - C_{i,P}\right) = \left(C_{i,b} - C_{i,P}\right).\exp\frac{J. \, l_{bl}}{D_{ji}} \tag{6}$$

The subscripts M, b, and p refer to the membrane surface, bulk and permeate respectively. In Equation (5), the term (D_{ji}/l_{bl}) is defined as the mass transfer coefficient $k_{i,b}$. If the permeate flux is based on a limited mass transport and the diffusion is Brownian, then the back diffusivity for small colloids and macromolecules may be calculated from the Stokes-Einstein Equation (7), as follows:

$$D_S = \frac{KT}{6\pi\mu r_p}$$ (7)

where K is Boltzmann constant, T is the absolute temperature, r_p is the particle radius, and μ is the solution viscosity.

The curvature of the concentration profile depends on the flux and so does the relationship between the mass transfer coefficients [19]. The mass transfer coefficient may be obtained from experiments using Equation (8), which is rearranged from Equation (6) with the assumption that the solute concentration in the permeate is very small compared to that of the feed and that at the membrane surface.

$$J = k_{i,b} \cdot \ln\left(\frac{C_{i,M}}{C_{i,b}}\right)$$ (8)

The mass transfer boundary layer thickness is equal to $D_{ji}/k_{i,b}$. When D_{ji} is small compared to the mass transfer coefficient $k_{i,b}$, the boundary layer is thin, especially for macromolecules. D_{ji} is exceedingly small and the boundary layer is thus very thin [20]. This causes severely localized high solute concentration at the membrane surface, which facilitates fouling.

Furthermore, fouling may be due to adsorption, pore blockage, deposition, and gel layer formation. The adsorption occurs whenever there are interactions between the membrane and the solute or particles. If the degree of adsorption is concentration-dependent, then the CP exacerbates the amount of adsorption creating an extra transport resistance [1]. Notably, the monolayer of particles and solute leads to an additional hydraulic resistance. The membrane surface hydrophilicity is the primary factor affecting particle-to-membrane attachments [21–23]. The deposit of particles can grow thicker by additional layers on top of the membrane's surface, leading to a significant hydraulic resistance, often referred to as a cake resistance. For certain macromolecules, CP may lead to gel formation in the immediate vicinity of the membrane surface. Furthermore, the size of contaminated particles plays a major role in the membrane pore blockage, which leads to a reduction in flux due to the partial closure of pores [5, 6]. In general terms, membrane fouling models are concerned with the non-dissolved materials that are either deposited on the membrane surface, or deposited in the membrane pores.

4. Modeling of porous membrane filtration in the presence of fouling

Membrane fouling provides additional transport resistance during the separation process. As a consequence, permeate flux and TMP are the best indicators of membrane fouling phenomenon [2]. The transport resistance created by the membrane fouling leads to a significant increase in hydraulic resistance, manifested as a permeate flux decline or TMP increase when the process is operated under constant-TMP or constant-flux conditions. The flux through most fouled membranes cannot be described by the idealized equation of Hagen-Poiseuille. It should also be noted that if a solute is present, then there will be CP. The following equation is used to describe the flux in the absence of any fouling cake layer:

$$J = \frac{\Delta p - \Delta \pi}{\mu R_m} \qquad (9)$$

where R_m is the empirically measured membrane resistance, Δp is the pressure drop, and $\Delta \pi$ is the osmotic pressure difference between upstream and downstream of the membrane. In general, the driving force ΔP that exists between the bulk feed on one side and the solution on the permeate side will be reduced by the osmotic pressure differences that occurs due to solute rejection. An alternative to Equation (9) can be defined as follows, with R_{cp} as the resistance of the CP layer:

$$J = \frac{\Delta p - \Delta \pi}{\mu \left(R_m + R_{cp} \right)} \qquad (10)$$

It was illustrated by Wijmans et al. (1985) that the two expressions are thermodynamically equivalent with the concentration boundary layer impeding the flow of the solvent and thus "consuming" part of the overall driving force [3]. While the value of $\Delta \pi$ can be calculated from equations for osmotic pressure of known concentration solutions, the value of R_{cp} can only be inferred from experimental data. Additional terms can be added to account for the hydraulic resistance that is caused by the material accumulation on the membrane's surface and/or in the membrane's pores, as shown in Equation (11). The pore diffusion transport model (PDTM) developed by Tu et al. (2005) allows to predict the flux decline and provides meaningful insight into the mechanisms affecting it. The model is intrinsically based on the presence of simultaneous fouling, being a joint function of CP, internal pore blocking, and gel or cake formation [19]. Although CP and internal pore fouling are effective factors for membrane fouling at the beginning of the filtration process however, according to PDTM surface fouling is insignificant since no gel layer is formed on the membrane's surface [24, 25]. A short time after the beginning of filtration, a gel layer is formed on the membrane surface due to the accumulation of the contaminated particles. At steady-state, no flux decline takes place due to the presence of a permanent gel layer. Equation (11) illustrates the overall hydraulic resistances, due to membrane fouling:

$$J = \frac{\Delta p - \Delta \pi}{\mu \left(R_m + R_{ads} + R_{irrev} \right)} \qquad (11)$$

The first of the additional hydraulic resistances, R_{ads}, is due to surface or pore adsorption that occurs independently of the flux. This resistance R_{ads} is estimated by measuring the permeate flux at a given TMP when the complete fouling occurs, after the estimation of membrane resistance R_m [26]. The increased resistance can be classified into reversible or irreversible based on the attachment strength of particles to the membrane surface. R_{ads} represents the sum of reversible and irreversible fouling. The reversible resistance occurs due to reversible fouling and disappears during the backwash process. On the other hand, the irreversible resistance, R_{irrev}, reflects the irreversible deposition after cleaning process. R_{cp} was insignificant in Equation (11).

When considering these fouling mechanisms, the critical flux, at which fouling is first observed for a given feed concentration and given crossflow velocity, should be a design consideration for all pressure-driven processes [27]. A model of critical flux, J_{cs}, has been developed in order to discriminate the un-fouling conditions (where R_m is the only resistance in Equation (11)) from fouling conditions where other resistances apply and the osmotic pressure is assumed negligible.

$$\text{For} < J_{cs} : J = \frac{\Delta p}{\mu R_m} \qquad (12)$$

$$\text{For} > J_{cs} : J = \frac{\Delta p}{\mu \left(R_m + \left(R_{rev} + R_{irrev} \right) \right)} \qquad (13)$$

For low J_{cs}, at least one of R_{rev} or R_{irrev} is non-zero and R_{ads} is considered to be negligible. For UF, the flux through the membrane can be described as analogous to that through a MF membrane with allowance for osmotic effects due to CP. The alternative form of the resistance-in-series model is presented in Equation (14).

$$J = \frac{\Delta p}{\mu \left(K_m + K_c + K_p \right)} \qquad (14)$$

where K_m, K_c, K_p are the resistance coefficient for membrane, cake layer, and pore constriction, and μ is Dynamic viscosity. The pore constriction resistance coefficient K_p can be negligible for small pore membranes such as NF. The resistance in a series model is a very useful and convenient concept to understand which resistance component is dominant and what should be performed in improving the flux. In bench scale studies, the cake layer

resistance coefficient K_c can be calculated using the Kozney equation for flow through a granular medium utilizing monodisperse spherical latex particle [27, 28]:

$$K_c = \frac{36\, K_K\, \delta_c \left(1-\varepsilon\right)^2}{\varepsilon^3 d_p^2} \tag{15}$$

where K_K [dimensionless] is Kozeny coefficient (typically 5), ε [dimensionless] is the cake porosity, δ_c [m] is the thickness of cake layer, and d_p [m] is the diameter of retained particles.

Several filtration models have been developed to describe the dynamics that frame the fouling process at a constant TMP. These models relate the permeate flow (Q), peremrate volume (V), the time (t) with the filtration constants for each model (K_{bc}, K_{ic}, K_{sc}, K_{dc}), and the initial permeate flow (Q_0). The mathematical expressions of these models and their assumptions are shown in Table 1.

Model	Equation	Assumption
Complete blocking filtration	$Q = Q_o - K_{bc} V$	Particles are not superimposed on one another; the blocked surface area is proportional to the permeate volume.
Intermediate blocking filtration	$\frac{1}{Q} = K_{ic} t + \frac{1}{Q_o}$	Particles can overlap each other; not every deposited particle block the pores.
Standard blocking filtration	$Q^{1/2} = Q_o^{1/2} - \left(\frac{K_{sc}\ V\ Q_o^{1/2}}{2}\right)$	Particles are small enough to enter the pores; the decrease of pore volume is proportional to the permeate volume.
Cake filtration	$\frac{1}{Q} = \frac{1}{Q_o} + K_{cc} V$	Particles are big enough to not enter the pores; and therefore forms a cake layer on the surface

Table 1. Constant pressure filtration model

Applications of these models were examined in numerous recent publications [29–33]. Lim investigated the fouling behavior of microfiltration membranes in an activated sludge system [29]. The results show that the main types of membrane fouling in this case were attributed to initial pore blocking (standard blocking filtration model) followed by cake formation (cake filtration model) [29]. Bolton (2006) compared these four models in application to microfiltration and ultrafiltration of biological fluids, the conclusion is the combined cake filtration model and the complete blocking model resulted in the best fit of experimental data [30]. In a cross flow ultrafiltration experiment conducted by Tarabara (2004), cake formation was investigated under variable particle size and solution ionic strength. The results revealed that in all cases,

there is a dense layer of the colloidal deposit adjacent to the membrane with an abrupt transition to a much more porous layer near the membrane-suspension interface [31]. This observation implies that different models should be considered at different phases of fouling.

5. Diffusion models in the presence of fouling

There is general consensus among research scholars that the solute mass transfer through RO and NF membranes is controlled by diffusion as a result of the concentration gradient across the membrane surface [34–38]. Researchers have invested extensive efforts in seeking new, comprehensive and accurate diffusion models capable of predicting membrane performance in cases involving membrane fouling. In most cases, the models were derived based on simplifications and assumptions, rendering limitation of the application of the models to practice. However, the diffusion models provide the basis and opportunity for incorporation of more complicated and realistic scenarios. Thus far, there is no universally accepted model for describing diffusion-controlled membrane processes, but understanding the factors affecting membrane mass transfer will certainly help with developing a better predictive model.

5.1. Homogeneous solution diffusion model (HSDM)

The homogeneous solution diffusion model (HSDM) is one of the basic models describing mass transfer as a function of concentration gradient and the pressure difference across the membrane's film. The HSDM assumes a homogeneous feed stream and homogeneous membrane surface that are linearly correlated to the average feed concentration and system recovery [39, 40]. This model is utilized to predict the permeate concentration, with a given solvent and solute mass transfer coefficient (MTC), overall recovery, transmembrane pressure, and feed concentration over a single element. The HSDM final formulation is given in Equation (16) [41, 42]:

$$C_p = \frac{k_s C_f}{F_W \left(\dfrac{2 - 2Rc}{2 - Rc} \right) + k_s} \tag{16}$$

where C_p is the permeate concentration, F_W is the water permeate flux, C_f is the feed concentration, k_s is solute MTC, and Rc is the overall recovery, which is the ratio of permeate flow rate to feed flow rate. The solute MTCs were found to be related to membrane feed water qualities and membrane properties. They can be theoretically determined using Fick's first law described in Equation (1) assuming a steady state within a thin film.

Duranceau (2011) developed a model correlating the solute MTCs to the solute charge and molecular weight with a normal distribution [41, 42]. Furthermore, Zhao (2005) investigated the influence of membrane surface properties and feed water qualities on solute MTCs. It was

found that the MTC increased as the surface roughness and contact angle were increased. Also, the amount of natural organic matter (NOM) in the feed water appeared to positively affect the MTC [35]. The HSDM has been modified to incorporate the osmotic pressure in an integrated incremental model by Zhao [38]. The model considered the osmotic pressure increase as a result of enhanced salt concentration in the membrane channel. Duranceau (2009) has modified the HSDM to predict multi-stage membrane systems [37]. Absar (2010) modified the diffusion model by comparing the effects of co-current and counter-current permeate flow with respect to the feed stream. It was concluded that the counter-current flow pattern, especially during the concentrating process, has a better overall efficiency [43].

5.2. Nonhomogeneous diffusion model development

Previous diffusion models had typically assumed a constant mass transfer rate across a non-porous, smooth, flat membrane surface. Nevertheless, the membrane surface characterization has been shown to affect the membrane's performance, as well as the overall fouling process [32, 33]. Therefore, non-homogeneous mass transfer model introduced an additional variable affecting mass transport that can be quantified by considering the non-uniform structure of the membrane surface. Research conducted by Mendret (2010) demonstrated that random distribution models may be used to effectively describe the heterogeneity of surfaces [28].

The HSDM can be modified by incorporating the effects of a non-uniform membrane surfaces on the solute permeability so as to obtain a non-homogeneous diffusion model. In addition, Sung (1993) has incorporated the film-theory factors accounting for the CP to develop the non-homogeneous diffusion model (NHDM), as presented in Equation (17)[39]. Notably, the k_s' is the back mass transfer coefficient was also incorporated:

$$C_p = \frac{C_f\, k_s'\, e^{F_W/k_s}}{k_W\,(\Delta p - \Delta \pi)\left(\dfrac{2-2Rc}{2-Rc}\right) + k_s'\, e^{F_W/k_s}}$$ (17)

where C_p [mg/L] is the solute concentration in the permeate, C_f is the feed concentration, k_s [m/s] is the solute mass transfer coefficient, k_W [m/s.psi] mass transfer coefficient and F_w [gal/sfd] is the solvent permeate flux. k_s is assumed to be related to the membrane surface morphology and therefore a variable parameter. Under laminar flow conditions, the back diffusion coefficient, ks, is related to the cross flow velocity and the geometry of the membrane channel [10]:

$$k_s' = 1.86\left(\frac{D}{d_h}\right)^{0.67}\left(v\right)^{0.33}$$ (18)

where k_s' [m/s] is the back diffusion mass transfer coefficient, d_h [m] is the hydraulic diameter of the membrane channel, v [m/s] is the cross flow velocity, and D [m²/s] is the salt diffusion

coefficient. The advantages of the non-homogeneous approach include the model's capacity to predict the hydraulic flow and solute concentration gradient in the bulk flow and on the membrane's surface, with a known solute concentration in the permeate. The overall back mass transfer coefficient was derived from a one-dimensional convective-diffusive mass balance, and was then integrated individually across the cake layer and the salt concentration boundary layer [27], as shown in Equation (19):

$$k_s' = \left[\delta_c \left(\frac{1}{D_s} - \frac{1}{D\infty} \right) + \frac{1}{k_s} \right]^{-1} \tag{19}$$

where δ_c is cake thickness, D_s is the back diffusivity, D^∞ is bulk diffusivity, and k_s is the solute mass transfer coefficient.

Mendret (2010) developed a model that considered two dimensional flow of a particle suspension in the membrane's channel in order to investigate the growth of a cake on a non-uniform permeability membrane [28]. The overall mass transfer coefficient (k_t) can be determined as below:

$$\frac{e_t}{k_t} = \frac{e_d}{k_d} + \frac{e_m}{k_m} \tag{20}$$

where e_t, e_d, e_m are the total thickness of the porous sub-domain, the deposit thickness, and the membrane thickness, and k_d, k_m are the deposit permeability and the membrane permeability, respectively.

The NHDM and HSDM were verified using pilot plant data from a brackish groundwater plant located in Florida. It was found that the NHDM predictions were in close agreement with actual permeate concentrations. The results likewise indicated that the NHDM provides a more accurate prediction of solute concentration with a high concentration in the feed stream. This can be explained by the role of CP effects on the mass transfer with different feed solute concentration, since the CP appears to be more significant in determining the salt passage in instances when the solute feed concentration is higher. Although it was found that the fouling behavior was related to the degree of surface roughness [2, 44–46], incorporating the surface roughness into the diffusion models and evaluating its impact has not been comprehensively studied yet.

6. Dimensionless mass transfer coefficient models

The mass transfer coefficient (k) is the most widely used parameter when it comes to the design of pressure-driven membrane separation systems. The mass transfer coefficient can be estimated from a dimensionless correlation using the Sherwood number [47]. Most models

used in the description of the CP phenomena during cross-flow membrane filtration require the knowledge of mass transfer coefficient [12]. Such an expression of the mass transfer coefficient should be able to represent the effects of changing conditions in the systems that are being used for membrane filtration. The value of the mass transfer coefficient k can be calculated using Sherwood relations [47, 48], generally represented as:

$$\text{Sh} = \frac{k\, d_h}{D} = \text{B}\, Re^q Sc^r \tag{21}$$

where d_h is the hydraulic diameter of the system; D is the diffusion coefficient; Re is the Reynolds number; S_C is the Schmidt number; and B, q, and r are the adjustable parameters. Usually, the description of the mass transfer coefficient is given for laminar and turbulent conditions separately. In literature, a number of different values for B, q, and r can be found depending on the operating conditions (laminar/turbulent conditions), the value of the Reynolds and Schmidt numbers [12]. The addition of the Sherwood relations to non-Newtonian fluids, as well as the laminar flow case, indicate that choosing a relationship that accurately describes a certain system is very difficult. The major limitations of such Sherwood number relationships include: (1) the failure to take into account the variations of physical properties (e.g., solution density, solute diffusivity, etc.) with concentrations due to concentration polarization; (2) the neglected effects of suction in the presence of a porous membrane; (3) the assumption that the mass transfer boundary layer is fully developed, which may not be the case in most of the conduits during macromolecular ultrafiltration (UF); and (4) the effects of pressure on the mass transfer coefficient, which may be present during ultrafiltration, have not been considered. Numerous Sherwood number relationships have been proposed and extensively reviewed [9]. In these reviews, it was identified that the standard correlations needed to be modified depending on the context of the limitations discussed earlier. In fact, it was suggested that alternative techniques, such as the velocity variation technique or the combined osmotic pressure-film theory model, may be utilized to estimate the mass transfer coefficient. However, both of these techniques have their respective disadvantages. To circumvent this problem a detailed numerical solution based on the governing momentum and solute mass balance equations with pertinent boundary conditions may be used [9]. But this method could appear problematic for design purposes due to certain inherent complexities and rigorous computational requirements. Another alternative approach proposes a second correlation for polarized layer resistance with operating conditions. However, such relationships are solute, system specific, and overall not general enough to encompass a wider variety of solute-membrane systems [3]. In addition, working with two correlations simultaneously increases the range of potential points of uncertainty and inaccuracy during the prediction.

Sirshendu and Bhattacharya [9] proposed new Sherwood number relationships that incorporate the effects of suction of a membrane for laminar flow in rectangular, radial, and tubular geometries. However, in this research study, the variations in physical properties brought about by concentration, and which become dominant under highly polarized conditions in a UF process, were not taken into consideration during the analysis. The large number of

experimental variables and corrections that are associated with the mass transfer relations provide a valid reason for directly determining the mass transfer coefficient experimentally [49]. Based on the data already available in the literature, the variables that have the capacity to influence the value of the mass transfer coefficient can be expected to include: the applied transmembrane pressure, the cross-flow velocity, the flux, the type of solute, the hydraulic dimensions of the module, and the characteristics of the membrane [48].

The commonly used Sherwood number correlation is that from Deissler, as shown in Equation (26). For solutes such as BSA and Dextrans (SC= 13,000-22,000), the mass transfer coefficient can be calculated from Harriott and Hamilton's equation [44].

$$1 << Sc <<1000 \left(\text{Deissler}\right); \; \text{Sh} = 0.023 \, Re^{0.875} Sc^{0.25} \tag{22}$$

$$Sc > 1000 \left(\text{Harriott} - \text{Hamilton}\right); \; \text{Sh} = 0.0096 \, Re^{0.91} \, Sc^{0.35} \tag{23}$$

6.1. The velocity variation method

The Sherwood relations for k, depending on the cross-flow velocity of the type $k = bv^a$, where "a" is about 0.33 for laminar conditions and around 0.75–0.91 for turbulent conditions. Therefore, to obtain the mass transfer coefficient an experimental based model was developed for the retention, as follows:

$$\ln\left[\frac{\left(1 - R_{obs}\right)}{R_{obs}}\right] = \ln\left[\frac{\left(1 - R\right)}{R}\right] + \frac{J}{(bv^a)} \tag{24}$$

where R_{obs} [dimensionless] is the observed retention coefficient and R is the intrinsic retention coefficient. By plotting the experimental values of $\ln\left[\frac{\left(1 - R_{obs}\right)}{R_{obs}}\right]$ as a function of J / v^a, where the value of the exponent (a) should be chosen in advance based on the flow regime, the intrinsic retention and the constant b can be determined graphically. The relation for the mass transfer coefficient as a function of the various experimental variables can then be obtained by accurately fitting the data found in the different experimental circumstances. A considerable disadvantage of this semi-empirical method is the necessity for an incomplete retention. While in practical circumstances for many solutes the retention is preferably complete and equal one, in this case the retention is relatively low.

The velocity variation method is not absolutely reliable when it comes to determining the mass transfer coefficient, primarily because its sensitivity to the experimental parameter values. The best experimental method for determining the mass transfer coefficient remains that of evaluation of the observed retention at varying velocities. Therefore, the use of normal mass transfer relations can be equally reliable and much easier than the velocity variation method [44]. The velocity variation method can be recommended for practice when one or more of the parameters in the conventional mass transfer coefficient relationships are unknown.

6.2. The modified Sherwood relation

The modified Sherwood number relationships, including the effects of suction during vacuum filtration and variations in properties brought about by concentration, may be a more adequate representation of concentration polarization phenomena during ultrafiltration of macromolecules [44]. Such a relationship is formulated for laminar flow in a rectangular geometry. The developed model is then employed to predict permeate flux of the ultrafiltration process of BSA and dextran. The value of the exponent in Equation (25) is found to be 0.01 for all operating conditions of BSA, and 0.013 for dextran at 5 kgm^{-3} and 0.026 at 10 kg m^{-3}. The present model is able to accommodate incomplete solute retention by the membrane and can be effectively applied during the simultaneous prediction of permeate flux and observed retention.

$$\text{Sh}_m = \text{Sh}\left(\frac{Sc}{Sc_m}\right)^n \tag{25}$$

7. Gas transport through membranes

A number of phenomenological and physiochemical models have been developed for gas transport, each of them suited specifically to particular types of penetrating membrane systems over limited pressure and temperature ranges [12]. Gas transport through membranes has been categorized as transport in homogeneous membranes, porous membranes, asymmetric, and composite membranes. The relationship between the permeation, flux, and operating conditions in general can be described by:

$$J = \frac{P}{L} \times \left(p_h - p_i\right) \tag{26}$$

where J is permeation flux, p_h is feed side pressure, p_i is permeate side pressure, P is permeability, L is membrane thickness.

The permeability value, P depends on the membrane material type and the variety of operating conditions used. Transport in homogeneous membranes can be assessed using the solution diffusion model (for rubbery polymer), Dual sorption model (for glassy polymer), and Free Volume Theory. The transport in porous membranes can be evaluated using the Pore model. On the other hand, transport in asymmetric and composite membranes, which are membranes that consist of several barrier layers with distinct nature, can be determined using the Resistance model [12]. Unlike asymmetric membranes, the composite membrane has a clear discontinuity at the boundary of two neighboring barrier layers, either in the chemical structure or in the morphology of the material.

The permeation rate, Q_i for a component i through a homogeneous membrane can be written as:

$$Q_i = J_i \times A = \frac{P}{L} \times A \times (p_h - p_i) = \frac{P}{L} \times A \times \Delta p \qquad (27)$$

In this case, the permeation rate, Qi, can be calculated as a function of the driving force, which is the pressure difference Δp and $R^{'}$ is the resistance to the flow, as in Equation (28):

$$Qi = \frac{\Delta p}{R'} \qquad (28)$$

The resistances in composite membranes are usually connected in a following manner: series, parallel, and two resistance arms. Two resistances are connected in series whenever two layers of membranes are combined in a series, as shown in Figure 3 (a). Two resistances are connected in parallel whenever the material of the membrane is different and connected along the same layer of the membrane's surface, as shown in Figure 3 (b). The parallel combination of two resistance models is used when a homogeneous film of relatively high permeability is laminated on top of the membrane, as shown in Figure 3 (c).
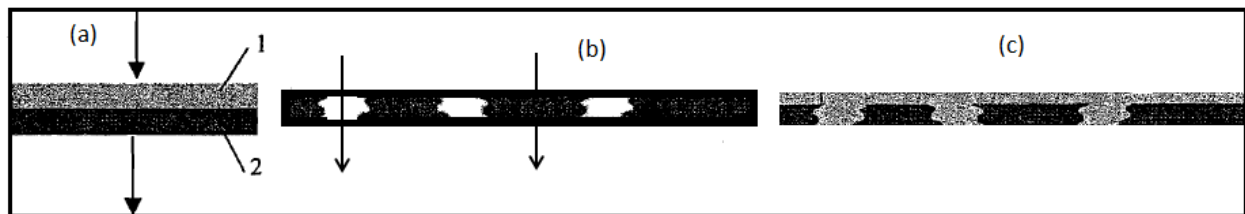
Figure 3. The connection of the transport resistances in composite membranes

The mass transport through a porous layer has been extensively studied. Its specific type depends on the pore size and its comparison to the mean path of the transported molecules. In the case of gas transport, three regions are distinguished regarding the transport [50]: (1) molecular and/or viscous flow, occurring when the mean free path of gas molecules is less than the pore size; (2) Knudsen diffusion, occuring when the pore size is larger than the size of transport species, but less than the mean free path of the gas molecule; and (3) molecular sieving transport (configurational diffusion), which tends to occur when the pore size is the same size as that of the transported species [51].

Molecular diffusion and/or viscous flow are dominated by the interaction between the transported molecules whenever the pore diameter is considerably larger than the mean free path. The viscous flow can be calculated according to Hagen-Poiseuille (Equation (2)), as illustrated in Equation (29):

$$J_i = v \frac{p_i}{RT} = -\frac{p_i}{RT} \frac{\varepsilon}{\tau} \frac{d_p^2}{32} \frac{dp}{dy} \qquad (29)$$

where p is the total pressure, p_i is the partial pressure and v is the convective velocity of the molecules. When both the molecular and the viscous flows exist, the total mass transfer rate is expressed through the sum of these two flow rates:

$$J_i = -\frac{1}{RT}\left(\frac{\varepsilon}{\tau}\frac{d_p^2}{32}p_i\frac{dp}{dy} + D_i\frac{dp_i}{dy}\right) \tag{30}$$

After integration, it can be obtained for the mass transfer rate:

$$J_i = \frac{1}{\delta}\left(\frac{\varepsilon}{\tau}\frac{d_p^2}{32}C_t + \frac{D_i}{RT}\right)(p_{e,i} - p_{t,i}) \tag{31}$$

where subscript e and t denote the feed side and the permeate side, and C_t is the total concentration (kmol/m³).

In case of Knudsen diffusion, flux can be calculated as follows:

$$J_i = -D_{K,i}\frac{dC_i}{dy} \equiv -\frac{D_{K,i}}{RT}\frac{dp_i}{dy} \tag{32}$$

where J_i is the mass transfer flux (kmol/m²s). The partial pressure gradient, dp_i/dy, is the driving force of the transport. The coefficient of Knudsen diffusion, $D_{K,i}$, can be estimated from [52]:

$$D_{K,i} = \frac{d_p}{3}\frac{\varepsilon}{\tau}\sqrt{\frac{8RT}{\pi M_i}} \tag{33}$$

where R is the gas constant, M_i is the molecular weight of species i (kg/kmol),and d_p is the pore size (m).

If the pore diameters approach the range comparable to that of the molecule sizes, then the configurational diffusion regime is reached [53]. The corresponding flux density can be described by [54]:

$$J_i = -\frac{1}{RT}\frac{\varepsilon}{\tau}D\frac{dp_i}{dz} \tag{34}$$

$$D = \rho_g d_p\sqrt{\frac{8RT}{\pi M_i}}\,e^{-(E_i^c/RT)} \tag{35}$$

where D is the diffusion coefficient (m^2/s) and E_i^c is activation energy of diffusion (kJ/kmol). There are no fully-accepted formulas available for the prediction of the diffusivity [53].

In the regions with very small pores compared with the solute molecular size, the effects of the surface diffusion might be significant. The surface diffusion flux can also be critical when it comes to the mass transport through pores in the Knudsen regime due to the adsorption [53, 54]. The most general approach for multicomponent surface diffusion was proposed by Krishna and Wesselingh [55]. Based on the physical picture of molecules moving on the surface, the generalized Maxwell À Stefan equations were applied so as to describe the interactions mechanistically [54, 55].

8. Conclusion

In membrane operations, there are several key issues that influence membrane separation and transport, which in turn affects the performance and the economy of the overall process. Membrane fouling is the major obstacle that inevitably decreases the membrane performance and cause flux decline due to the presence of external and internal membrane fouling. The understanding of causes of flux decline and the ability of predicting the flux performance is essential for more extensive membrane applications. Therefore, this review focused on the analysis of the interrelated dynamics of membrane fouling, flux decline, and mass transport in the filtration/separation process. In addition, this study illustrates that extensive efforts have been undertaken by many researchers to investigate various aspects of these complex phenomena. These studies form the foundation necessary for the alleviation of adverse effect of membrane fouling and emphasize the fact that the development of a complex overlapping approach is needed. Investigations of the mechanisms of mass transfer in high and low pressure membranes, analyses of diffusion mechanisms in membrane pores together with identifications of transport resistances resulting from membrane fouling will allow for a comprehensive understanding and in-depth knowledge of the fouling phenomenon and applicable mass transfer mechanism.

Several mathematical models have been developed over the years in order to describe the solute and solvent mass transport in membrane processes based on a homogeneous membrane surface. In addition, the effect of the morphology of the membrane active layer on solvent and solute mass transport was incorporated. It was determined that solute mass transport is controlled by the non-homogeneous diffusion in the thinner regions of the active layer. This non-uniform surface also affects the concentration polarization layer, where more solutes tend to accumulate on the valleys rather than on the ridges. The NHDM was developed, taking into account the membrane surface property, so as to describe the non-homogeneous phenomenon while accommodating the fact that solute and solvent MTCs vary with active layer thickness. Based on the same conceptual the dynamic model, which is a non-homogeneous diffusion model, was developed with and without the CP effect, and then compared with the HSDM. It was found that the mass transport across the membrane film was affected by the morphology of the membrane surface.

Nomenclature

Symbol	Physical Meaning
A	Cross-sectional area to flow [m²]
B	Constant depending on flow patterns [dimensionless]
C	concentration of diffusing substances [kg/m³]
$C_{i,\mathrm{M}}$	Concentration of solute i at the membrane surface [kg/m³]
$C_{i,\mathrm{b}}$	Concentration of solute i at the bulk [kg/m³]
$C_{i,\mathrm{p}}$	Concentration of solute i at the permeate [kg/m³]
C_f	Feed concentration [kg/m³]
D_{ji}	Diffusivity of component i [m²/s]
D_s	Back diffusivity [m²/s]
D^∞	Bulk diffusivity [m²/s]
d_{pore}	Diameter of the capillaries [m]
d_p	Diameter of retained particles [m]
d_h	Hydraulic diameter of the membrane channel [m]
E_i^c	Activation energy of diffusion [kJ/kmol]
e_t	Total thickness of the porous sub-domain [m]
e_d	Deposit thickness [m]
e_m	Membrane thickness [m]
F_w	Water permeate flux [m³/m²s]
J	Permeate flux [m³/m²s]
J_w	Permeate flux of pure water [m³/m²s]
k_m	Resistance coefficient for membrane
k_c	Resistance coefficient for cake layer
k_p	Resistance coefficient for pore constriction
k_k	Kozeny coefficient (typically 5) [dimensionless]
K	Permeability constant [m²]
$k_{i,b}$	Mass transfer coefficient [m/s]
k_d	Deposit permeability [m²]
k_s	Solute mass transfer coefficient [m/s]
$k_s{}'$	Back mass transfer coefficient [m/s]
K_{bc}	Filtration constant of complete blocking model [dimensionless]

Symbol	Physical Meaning
K_{ic}	Filtration constant of intermediate blocking model [dimensionless]
K_{sc}	Filtration constant of standard blocking model [dimensionless]
K_{dc}	Filtration constant of cake model [dimensionless]
K	Boltzman constant [dimensionless]
L	Membrane thickness [m]
l_{pore}	Thickness of the porous layer [m]
l_{bl}	Thickness of the mass transfer boundary layer [m]
μ	Dynamic viscosity of the permeate [kg/(m·s) or Pa·s]
ΔP	Pressure drop [psi]
$(P_b - P_a)$	Pressure drop [psi]
P	Permeability [m²]
Q	Total discharge [m³/s]
Q_0	Initial permeate flow [m³/s]
q	Constant depending on flow patterns [dimensionless]
Re	Reynolds number [dimensionless] $\left(\rho v L / \mu \right)$
r	Constant depending on flow patterns [dimensionless]
r_p	Particle radius [m]
R_m	Membrane resistance [m⁻¹]
R_{cp}	Resistance of the concentration polarization layer [m⁻¹]
R_{ads}	Hydraulic resistances, due to surface or pore adsorption [m⁻¹]
R_{irrev}	Irreversible resistance due to irreversible deposition [m⁻¹]
Rc	Overall recovery [%]
R_{obs}	Observed retention coefficient [dimensionless]
R	Intrinsic retention coefficient [dimensionless]
R'	Resistance to flow
R	Gas constant [J/mol. K]
S	Specific area per unit volume [m²/m³]
Sc	Schmidt number [dimensionless] $(\mu / \rho L)$
Sh	Sherwood number [dimensionless] $\left(kL / D \right)$
T	Absolute temperature [K]
τ	Tortuosity of the capillaries [dimensionless]
t	Filtration time [seconds]

Symbol	Physical Meaning
V	Permeate volume [m^3]
v	Cross-flow velocity [m/s]
Z	Space coordinate measured normal to the membrane [dimensionless]
$\Delta\pi$	Osmotic pressure [atm]
$\Delta\pi_m{}^*$	Osmotic pressure difference [atm]
ε	Surface porosity [dimensionless]
δ_c	Thickness of cake layer [m]

Author details

Amira Abdelrasoul*, Huu Doan, Ali Lohi and Chil-Hung Cheng

*Address all correspondence to: amira.abdelrasoul@ryerson.ca

Department of Chemical Engineering, Ryerson University, Toronto, Ontario, Canada

References

[1] Gekas V, Hallstrom B. Mass transfer in the membrane concentration polarization layer under turbulent cross flow, Critical literature review and adaptation of existing Sherwood correlations to membrane operations. *J. Membr. Sci.* 1987;80:153–170.

[2] Abdelrasoul A, Doan H, Lohi A. Fouling in membrane filtration and remediation methods. *Mass Transfer - Advances in Sustainable Energy and Environment Oriented Numerical Modeling*, Dr. Hironori Nakajima (Ed.). Intech Open Access Publisher. 2013;195–218.

[3] Wijmans JG, Nakao S, Van Den Berg J, Troelstra FR, Smolders CA. Hydrodynamic resistance of concentration polarization boundary layers in ultrafiltration. *J.Membr. Sci.* 1985;22:117–135.

[4] Vasan SS, Field RW. On maintaining consistency between the film model and the profile of the concentration polarisation layer. *J. Membr. Sci.* 2006;279:434–438.

[5] Abdelrasoul A, Doan H, Lohi A. A mechanistic model for ultrafiltration membrane fouling by latex. *J. Membr. Sci.* 2013;433:88–99.

[6] Abdelrasoul A, Doan H, Lohi A, Cheng CH. Modeling development for ultrafiltration membrane fouling of heterogeneous membranes with non-uniform pore size. *Can. J. Chem. Eng.* 2014;92 (11):1926–1938.

[7] Jennifer A. Model studies of diffusion-controlled (2-hydroxyethyl methacrylate) HE-MA hydrogel membranes for controlled release of proteins, State University of New York at Buffalo, 2012;327.

[8] Mirando J, Campos J. Mass transfer in the vicinity of a separation membrane the applicability of the stagnant film theory. *J. Membr. Sci.* 2002;202:137–150.

[9] Sirshendu D, Bhattacharya P. Mass transfer coefficient with suction including property variations in applications of cross-flow ultrafiltration. *Sep. Purif. Technol.* 1999;16:61–73.

[10] Fang Y. Study of the effect of surface morphology on mass transfer and fouling behavior of reverse osmosis and nanofiltration membrane processes, University of Central Florida, Orlando, Florida, 2013.

[11] Lonsdale HK. The growth of membrane and technology. *J. Membr. Sci.* 1982;11:81–181.

[12] Nagy E. *Basic Equations of the Mass Transport through a Membrane Layer*, Elsevier, 2012.

[13] Bird RB, Stewart W, Lightfoot EN. Transport phenomena, John Wiley and Sons, New York, 1960.

[14] Geankoplis CJ. Transport processes and separation process principles, 4th ed. Prentice Hall, New Jersey, 2003.

[15] Goosen M, Sablani S, Al-Maskari S, Al-Belushi R, Wilf M. Effect of feed temperature on permeate flux and mass transfer coefficient in spiral-wound reverse osmosis systems. *Desalination*. 2002;144:367–372.

[16] Duranceau S, Taylor J. Solute charge and molecular weight modeling for predicting of solute MTCs. Proceedings AWWA MTC. Baltimore, MD, 1993.

[17] Merten U. Transport Properties of Osmotic Membranes, *Desalination by Reverse Osmosis*, U.

[18] Merten, ed., pp. 15–54, MIT Press, Cambridge, Mass. 1966.

[19] Morineau-Thomas O, Jaouen P, Legentilhomme P. Modeling of fouling in three ultrafiltration cell configurations: Swirl, plane and axial annular. *Chem. Eng. Technol*. 2001;24:1521–4125.

[20] Tu SC, Ravindran V, Pirbazari M. A pore diffusion transport model for forecasting the performance of membrane processes. *J. Membr. Sci.* 2005;265 29–50.

[21] Coskun A, Yasemin K, Zeren B, Vergili I. Evaluation of membrane fouling and flux decline related with mass transport in nanofiltration of tartrazine solution. *J. Chem. Technol. Biotechnol.* 2010;85:1229–1240.

[22] Abdelrasoul A, Doan H, Lohi A, Cheng CH. Modeling of fouling and foulant attachments on heterogeneous membranes in ultrafiltration of latex solution. *Sep. Purif. Technol.* 2014;135:199–210.

[23] Abdelrasoul A, Doan H, Lohi A, Cheng CH. Modeling of fouling and fouling attachments as a function of the zeta potential of heterogeneous membranes surfaces in ultrafiltration of latex solution. *Ind.& Eng. Chem. Res.* 2014;53: 9897–9908.

[24] Benitez F, Acero J, Leal A, Gonzalez M. The use of ultrafiltration and nanofiltration membranes for the purification of cork processing wastewater. *J. Hazard. Mater.* 2009;162:1438–1445.

[25] Field RW, Wu D, Howell J, Gupta B. Critical flux concept for microfiltration fouling. *J. Membr. Sci.* 1995;100:259–272.

[26] Bacchin P, Aimar P, Field R. Critical and sustainable fluxes fundamentals of fouling review: Theory, experiments and applications. *J. Membr. Sci.* 2006;281:42–69.

[27] Zhao Y, Taylor J. Assessment of ASTM D4516 for evaluation of reverse osmosis membrane performance. *Desalination.* 2005;180:231-244.

[28] Mohammadi T, Kazeminoghadam M, Saadabadi M. Modeling of membrane fouling and flux decline in reverse osmosis during separation of oil in water emulsions. *Desalination.* 2003;157:369–375.

[29] Mendret J, Guigui C, Cabassud C. Numerical investigation of the effect of non-uniform membrane permeability on the deposit formation and filtration process. *Desalination*. 2010;263:122–132.

[30] Lim A, Bai R. Membrane fouling and cleaning in microfiltration of activated sludge wastewater. *J. Membr. Sci.* 2003;216:279–290.

[31] Bolton G, LaCasse D, Kuriyel R. Combined models of membranes fouling: Development and application to microfiltration and ultrafiltration of biological fluids. *J. Membr. Sci.* 2006;277(1–4):75–84.

[32] Tarabara V, Koyuncu I, Wiesner M. Effect of hydrodynamics and solution ionic strength on permeate flux in cross-flow filtration: Direct experimental observation of filter cake cross-sections. *J. Membr. Sci.* 2004;241(1):65–78.

[33] Sioutopoulos S, Yiantsios DG, Karabelas AJ. Relation between fouling characteristics of RO and UF membranes in experiments with colloidal organic and inorganic species. *J. Membr. Sci.* 2010;350:62–82.

[34] Belfort G, Davis R, Zydney A. The behavior of suspensions and macromolecular solutions in crossflow microfiltration. *J. Membr. Sci.* 1994;96(28):1–58.

[35] ZhaoY, Taylor J. Combined influence of membrane surface properties and feed water qualities on RO/NF mass transfer, a pilot study. *Water Res.* 2005;39:1233–1244.

[36] ZhaoY, Taylor J. Incorporation of osmostic pressure in an integrated incremental model for predicting RO or NF permeate concentration. *Desalination.* 2005;174:145–159.

[37] Jamal K, Khan MA, Kamil M. Mathematical modelin of reverse osmosis system. *Desalination.* 2004;160:29–42.

[38] Duranceau S. Modeling the permeate transient response to perturbation from steady state in a nanofiltration process. *Desalin. Water Treat.* 2009;1:7–16.

[39] Zhao Y, Taylor JS, Chellam S. Predicting RO/NF water quality by modified solution diffusion model and artificial neural networks. *J. Membr. Sci.* 2005;263:38–46.

[40] Sung LK. *Film-theory and ion coupling models for diffusion controlled membrane processes.* Ph.D dissertation: University of Central Florida, 1993.

[41] Taylor J, Jacob EP. *Reverse osmosis and nanofiltration in water treatment membrane Processes*, McGraw-Hill, 1996, Chapter 9.

[42] Duranceau S, Taylor JS. Membranes. In J. Edzwald, Water Quality and Treatment. Denver, Colorado: American Water Works Association, 2011, Chapter 11, 11.4–11.9.

[43] Duranceau S. *Modeling of mass transfer and synthetic organic compound removal in a membrane softening process.* Ph.D dissertation: University of Central Florida, 1990.

[44] Absar B, Belhamiti O. Reverse osmosis modeling with orthogonal collocation of finite element method. *Desalin. Water Treat.* 2010;21:23–32.

[45] Boussu K, Brlpaire A, Volodin A, Haesendonck C, Van der Meeren P, Vandecasteele C. Influence of membrane and colloid characteristics on fouling of nanofiltration membranes. *J. Membr. Sci.* 2007;289:220–230.

[46] Norberg D, Hong S, Taylor J, Zhao Y. Surface characterization and performance evaluation of commercial fouling resistant low-pressure RO membranes. *Desalination.* 2007;2002:45–52.

[47] Warsinger DM, Swaminathan J, Guillen-Burrieza E, Arafat HA, Lienhard JH. Scaling and fouling in membrane distillation for desalination applications: A review. *Desalination.* 2014;356:1–20.

[48] Sherwood TK, Brian P, Fisher R, Dresner L. Salt concentration at phase boundaries in desalination by reverse osmosis. *Ind. & Eng. Chem. Fundamentals.* 1965;4:113–118.

[49] Crittenden JC, Trussell R, Hand DW. *Water Treatment Principles and Design*. New Jersey: Jonh Wiley & Sons. Inc, 2012.

[50] Berg GB, Racz IG, Smolders CA. Mass Transfer Coefficients in cross flow ultrafiltration. *J. Membr. Sci.* 1989;47:25–51.

[51] Seidel-Morgenstern A. *Membrane Reactors*. Wiley-VCH, Weinheim, 2010.

[52] Lawson KW, Lloyd DR. Membrane distillation: Review. *J. Membr. Sci.* 1997;124:1–25.

[53] Mason EA, Malinauskas AP. *Gas Transport in Porous Media: The Dusty Gas Model*. Elsevier, Amsterdam, 1983.

[54] Thomas S, Schafer R, Caro J, Seidel-Morgenstern A. Investigation of mass transfer through inorganic membrane with several layers. *Catalysis Today.* 2001;67:205–216.

[55] Tuchlenski A, Uchytil P, Seidel-Morgenstern A. An experimental study of combined gas phase and surface diffusion in porous glass. *J. Membr. Sci.* 2001;140:165–184.

[56] Krishna R, Wesselingh JA. The Maxwell-Stefan approach to mass transfer. Chem. Eng. Sci. 1997;52:861–911.